
Fragment-Based Sequential Translation for Molecular Optimization

Anonymous Author(s)

Affiliation

Address

email

Abstract

1 Search of novel molecular compounds with desired properties is an important
2 problem in drug discovery. Many existing generative models for molecules operate
3 on the atom level. We instead focus on generating molecular fragments—meaningful
4 substructures of molecules. We construct a coherent latent representation for
5 molecular fragments through a learned variational autoencoder (VAE) that is
6 capable of generating diverse and meaningful fragments. Equipped with the
7 learned fragment vocabulary, we propose **F**ragment-based **S**equential **T**ranslation
8 (FaST), which iteratively translates model-discovered molecules into increasingly
9 novel molecules with high property scores. Empirical evaluation shows that FaST
10 achieves significant improvement over state-of-the-art methods on benchmark
11 single-objective/multi-objective molecular optimization tasks.

12 1 Introduction

13 Molecular optimization is a challenging task for drug discovery, and has been explored in previous
14 work through several different generation methods, including VAE [5, 15], GAN [10], and RL
15 [6]. These character-by-character (for SMILES/SELFIES strings) and node-by-node (for molecular
16 graphs) models generate valid molecules, but can struggle to explore the complex chemical space
17 under multiple property constraints. More recent works attempt to generate molecules using a
18 predefined set of fragments [20, 13, 19] and achieve impressive empirical results. However, the fixed
19 fragment vocabulary limits the generative capabilities of the models.

20 Shifting away from previous frameworks, we learn a distribution of molecular fragments using vector-
21 quantized variational autoencoders (VQ-VAE) [18]. We then generate molecular graphs through
22 addition and deletion of molecular fragments from the learned distributional fragment vocabulary,
23 enabling the generative model to span a much larger chemical space than models with a fixed fragment
24 vocabulary. Considering atomic edits as primitive actions, the idea of using fragments can be thought
25 of as *options* [17, 16] as a way to simplify the search problem.

26 There are two primary generation schemes from previous works: (1) generating from scratch [20, 19]
27 and (2) translating from known active molecules [8, 7]. Generation under the first scheme is usually
28 very challenging because the set of molecules with high property score is typically a very small
29 subspace of the entire chemical space. It is, in general, much easier to generate molecules satisfying
30 desired properties under the translation scheme, being able to start from a prior over “good” molecules.
31 However, this generation scheme suffers from generating molecules too similar to those in the active
32 set, which is undesirable as this precludes the ability of the model to produce novel molecules for
33 drug discovery applications.

34 To this end, we bridge the gap between the two aforementioned generation paradigms by introducing
35 a novel *sequential translation* scheme. We start the molecular search by translating from known active

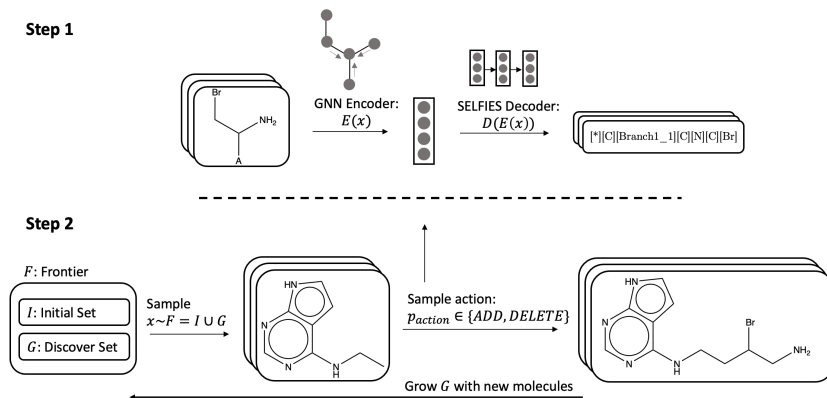


Figure 1: Overview of **F**ragment-based **S**equential **T**ranslation (FaST), which consists primarily of two component steps. In the first step, we train a VQ-VAE that embeds molecular fragments. In the second step, we train a search policy that uses the learned embeddings as an action space. The search policy starts from the *frontier* set F , which consists of an initial set of good molecules (I), and good molecules discovered by the policy (G).

36 molecules, and store the discovered molecules as new potential initialization states for subsequent
 37 searches. As monotonic expansion of molecular graphs will end up producing undesirable, large
 38 molecules, we also include the deletion of fragments as a possible action. This enables our method to
 39 backtrack to good molecular states, and iteratively improve generated molecules during the sequential
 40 translation process. Our proposed framework is (1) highly efficient in finding molecules that satisfy
 41 property constraints since the model stay close to the high-property-score chemical manifold; and (2)
 42 able to produce highly novel molecules because the sequence of fragment-based translation can lead
 43 to very different and diverse molecules compared to the known active set.

44 2 Methods

45 **Molecular Optimization as a Markov Decision Process.** We model the molecular optimization
 46 problem as a Markov decision process (MDP), defined by the 5-tuple $\{\mathcal{S}, \mathcal{A}, p, r, \rho_0\}$, where the
 47 state space \mathcal{S} is the set of all molecules. The goal of molecular optimization is to find a set of
 48 molecules $G \subset \mathcal{S}$ that has high quality (success), novelty, and diversity (detailed in Section 3). In
 49 order to achieve this goal, we introduce novel designs over the action space \mathcal{A} (and the corresponding
 50 transition model $p : \mathcal{S} \times \mathcal{A} \rightarrow \mathcal{S}$), the reward function r and the initial state distribution ρ_0 . In
 51 summary, our action space \mathcal{A} is based on molecular fragments learned by a VQ-VAE, while r and ρ_0
 52 interact with policy learning to implement the proposed sequential translation optimization scheme.
 53 An illustration of our model is in Figure 1.

54 2.1 Fragment-based Molecular Generation

55 **VQ-VAE Encoder/Decoder** We first pretrain a VQ-VAE on molecular fragments, which uses a
 56 GNN encoder. GNNs are suitable for describing actions on the molecular state, as they explicitly
 57 parametrize the representations of each atom and bond. Meanwhile, the decoder architecture is a
 58 recurrent network that decodes a SELFIES string representation of a molecule. We choose a recurrent
 59 network for the decoder, because we do not need the full complexity of a graph decoder. Due to
 60 the construction scheme (see Appendix A.2), the fragments are rooted trees and all have a single
 61 attachment point. As our fragments are small in molecular size (≤ 10 atoms), the string grammar is
 62 simple to learn, and we find the SELFIES decoder works well empirically.

63 **Adding and deleting fragments as actions.** At each step of the MDP, the policy network first
 64 takes the current molecular graph as input and produce a Bernoulli distribution on whether to add or
 65 delete a fragment. Equipped with the fragment VQ-VAE, we define the *Add* and *Delete* actions at the
 66 fragment-level:

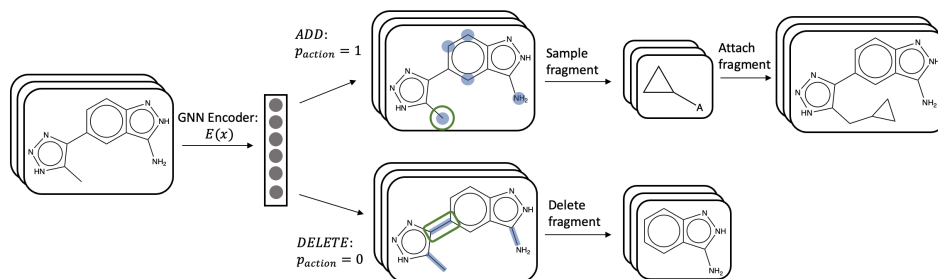


Figure 2: Each episode starts from a molecule sampled from the frontier. The molecule is encoded by a GNN, which is then used to predict either an *Add* or *Delete* action. When the *Add* action is selected, the model predicts and samples an atom as the attachment point, and subsequently predicts a fragment to attach to that atom. When the *Delete* action is selected, the model samples a directed edge, indicating the molecular fragment to be deleted.

- 67 • **Fragment Addition.** The addition action is characterized by a probability distribution over
 68 the atoms: $p_{add}(v_i) = \sigma[\text{MLP}(h_v)]$, where h_v is the output atom embedding of the GNN.
 69 Conditioned on the attachment point atom v_{add} sampled from p_{add} , we predict a categorical
 70 latent vector that is fed to the decoder: $z_{add} = \sigma[\text{MLP}([h_{v_{add}}; h_x])]$, where h_x is the
 71 embedding of the input molecular graph. The fragment to add is then obtained by decoding
 72 z_{add} through the learned fragment decoder.
- 73 • **Fragment Deletion.** The deletion action acts over the directed edges of the molecule.
 74 A probability distribution over deletable edges is computed with a MLP: $p_{del}(e_{ij}) =$
 75 $\sigma[\text{MLP}(h_{e_{ij}})]$, where $h_{e_{ij}}$ is the final edge embedding for edge e_{ij} . One edge is then
 76 sampled and deleted; since the edges are directed, the directionality specify the the molecule
 77 to keep and the fragment to be deleted.

78 With the action space \mathcal{A} defined as above, the transition model for the MDP is simply $p(s'|s, a) = 1$
 79 if applying the addition/deletion action a to s results in the molecule s' , and $p(s'|s, a) = 0$ otherwise.
 80 We terminate an episode when the molecule fails to satisfy the desired property or when the episode
 81 exceeds 10 steps. The fragment-based action space is powerful as it (1) is powered by the enormous
 82 distributional vocabulary learned by the fragment VQ-VAE, thus spans a diverse set of editing
 83 operations over molecular graphs; (2) exploits the meaningful latent representation of fragments,
 84 since the representation of similar fragments are grouped together. These advantages greatly simplify
 85 the molecular search problem. An illustration of the two types of actions is given in Figure 2.

86 2.2 Discover Novel Molecules through Sequential Translation

87 We propose sequential translation that incrementally grows the set of discovered novel molecules,
 88 and uses the model-discovered molecules as starting points for further search episodes. This regime
 89 of starting exploration from states reached in previous episodes was also explored under the setting of
 90 RL from image inputs [2]. More concretely, we implement sequential translation with a reinforcement
 91 learning policy that operates under the fragment-based action space defined in Section 2.1, while
 92 using a moving initial state distribution ρ_0 , which is a distribution over the *frontier* set F – the union
 93 of the initial set and good molecules that are discovered by the RL policy. We gradually expand
 94 the discovered set G by adding *qualified* molecules found in the RL exploration within the MDP. A
 95 molecule is qualified if it satisfies the desired properties and is novel compared to molecules currently
 96 in the frontier F , measured by fingerprint similarity. We use a simple binary reward of +1 for a
 97 transition that results in a molecule qualified for the set G , and a reward of 0 otherwise. We further
 98 discourage the model from producing invalid molecules by adding a reward of -0.1 for a transition
 99 that produces an invalid molecular graph. We further use an upper-confidence-bound (UCB) score to
 100 select good initial molecule from the frontier set. More implementation details of the method are
 101 included in the appendix.

Table 1: Results on our model (FaST) against multiple baselines. FaST outperforms all the baselines on both single-property optimization and multi-property optimization.

| Model | GSK3 β | | | | GSK3 β +QED+SA | | | |
|----------------|--------------|------|------|-------------------------------------|----------------------|------|------|-------------------------------------|
| | SR | Nov | Div | PM | SR | Nov | Div | PM |
| Rationale-RL | 1.00 | .534 | .888 | .474 | .699 | .402 | .893 | .251 |
| GA+D | .846 | 1.00 | .714 | .600 | .891 | 1.00 | .628 | .608 |
| JANUS | 1.00 | .829 | .884 | .732 | - | - | - | - |
| MARS | 1.00 | .840 | .718 | .600 ($\pm .04$) | .995 | .950 | .719 | .680 ($\pm .03$) |
| MARS+Rationale | .995 | .804 | .746 | .597 ($\pm .07$) | .981 | .800 | .807 | .632 ($\pm .07$) |
| FaST | 1.00 | 1.00 | .905 | .905 ($\pm .000$) | 1.00 | 1.00 | .861 | .861 ($\pm .001$) |

| Model | JNK3 | | | | JNK3+QED+SA | | | |
|----------------|------|------|------|-------------------------------------|-------------|------|------|-------------------------------------|
| | SR | Nov | Div | PM | SR | Nov | Div | PM |
| Rationale-RL | 1.00 | .462 | .862 | .400 | .623 | .376 | .865 | .203 |
| GA+D | .528 | .983 | .726 | .380 | .857 | .998 | .504 | .431 |
| JANUS | 1.00 | .426 | .895 | .381 | - | - | - | - |
| MARS | .988 | .889 | .748 | .660 ($\pm .04$) | .913 | .948 | .779 | .674 ($\pm .02$) |
| MARS+Rationale | .976 | .843 | .780 | .642 ($\pm .04$) | .634 | .779 | .787 | .386 ($\pm .08$) |
| FaST | 1.00 | 1.00 | .905 | .905 ($\pm .001$) | 1.00 | .866 | .856 | .741 ($\pm .001$) |

| Model | GSK3 β +JNK3 | | | | GSK3 β +JNK3+QED+SA | | | |
|----------------|--------------------|------|------|-------------------------------------|---------------------------|------|------|-------------------------------------|
| | SR | Nov | Div | PM | SR | Nov | Div | PM |
| Rationale-RL | 1.00 | .973 | .824 | .800 | .750 | .555 | .706 | .294 |
| GA+D | .847 | 1.00 | .424 | .360 | .857 | 1.00 | .363 | .311 |
| JANUS | 1.00 | .778 | .875 | .681 | 1.00 | .326 | .821 | .268 |
| MARS | .995 | .753 | .691 | .520 ($\pm .08$) | .923 | .824 | .719 | .547 ($\pm .05$) |
| MARS+Rationale | .976 | .843 | .780 | .642 ($\pm .04$) | .654 | .687 | .724 | .321 ($\pm .09$) |
| FaST | 1.00 | 1.00 | .863 | .863 ($\pm .001$) | 1.00 | 1.00 | .716 | .716 ($\pm .011$) |

102 3 Experiments

103 **Datasets, evaluation, and baselines.** We use benchmark datasets for molecular optimization,
 104 which aims to generate ligand molecules for inhibition of two proteins: glycogen synthase kinase-3
 105 beta (GSK3 β) and c-Jun N-terminal kinase 3 (JNK3). We also optimize for quantitative estimate of
 106 drug-likeness (QED) [1] and synthetic accessibility (SA) [3] as done in previous work. Following
 107 previous works, we evaluate our generative model on three target metrics, success, novelty and
 108 diversity. The metric scores are computed from 5,000 molecules generated by the model. Our model
 109 is initialized with molecule rationales as obtained in Jin et al. [8]. We compare to state-of-the-art
 110 molecular optimization methods including **Rationale-RL** [8] (molecular rationales as initialization +
 111 atom-by-atom RL completion); **GA+D & JANUS** [11, 12] (genetic algorithms); and **MARS** [19] &
 112 **MARS+Rationale** (MCMC sampler initialized with/without rationales). More details on the datasets,
 113 evaluation metrics, and baseline methods are included in the appendix.

114 **Performance** FaST outperforms all the baselines on all tasks including both single-property and
 115 multi-property optimization. For the most challenging task, GSK3 β +JNK3+QED+SA, our model
 116 improves upon the previous best model by over 30% in the product of the three evaluation metrics.
 117 The MARS+Rationale model, which uses the same rationale molecules as the initialization for their
 118 search algorithm, does not perform well compared to the original implementation, which initializes
 119 each search with a simple "C-C" molecule. Our model is able to efficiently search for molecules that
 120 stay within the constrained property space, and discover novel and diverse molecules by sequentially
 121 translating known active molecules.

122 4 Conclusion

123 We propose a new framework for molecular optimization, which leverages a learned representation of
 124 molecular fragments to search the chemical space efficiently. We demonstrate that our search method,
 125 which adaptively grows a set of promising molecular candidates, can achieve high performance on
 126 single-property and multi-property optimization tasks.

References

- 127
- 128 [1] G Richard Bickerton, Gaia V Paolini, Jérémy Besnard, Sorel Muresan, and Andrew L Hopkins.
129 Quantifying the chemical beauty of drugs. *Nature chemistry*, 4(2):90–98, 2012. 4
- 130 [2] Adrien Ecoffet, Joost Huizinga, Joel Lehman, Kenneth O Stanley, and Jeff Clune. First return,
131 then explore. *Nature*, 590(7847):580–586, 2021. 3
- 132 [3] Peter Ertl and Ansgar Schuffenhauer. Estimation of synthetic accessibility score of drug-like
133 molecules based on molecular complexity and fragment contributions. *Journal of cheminform-*
134 *atics*, 1(1):1–11, 2009. 4
- 135 [4] Anna Gaulton, Louisa J Bellis, A Patricia Bento, Jon Chambers, Mark Davies, Anne Hersey,
136 Yvonne Light, Shaun McGlinchey, David Michalovich, Bissan Al-Lazikani, et al. ChEMBL: a
137 large-scale bioactivity database for drug discovery. *Nucleic acids research*, 40(D1):D1100–
138 D1107, 2012. 7
- 139 [5] Rafael Gómez-Bombarelli, Jennifer N Wei, David Duvenaud, José Miguel Hernández-Lobato,
140 Benjamín Sánchez-Lengeling, Dennis Sheberla, Jorge Aguilera-Iparraguirre, Timothy D Hirzel,
141 Ryan P Adams, and Alán Aspuru-Guzik. Automatic chemical design using a data-driven
142 continuous representation of molecules. *ACS central science*, 4(2):268–276, 2018. 1
- 143 [6] Gabriel Lima Guimaraes, Benjamin Sanchez-Lengeling, Carlos Outeiral, Pedro Luis Cunha
144 Farias, and Alán Aspuru-Guzik. Objective-reinforced generative adversarial networks (organ)
145 for sequence generation models. *arXiv preprint arXiv:1705.10843*, 2017. 1
- 146 [7] Wengong Jin, Kevin Yang, Regina Barzilay, and Tommi Jaakkola. Learning multimodal
147 graph-to-graph translation for molecule optimization. In *International Conference on Learning*
148 *Representations*, 2019. URL <https://openreview.net/forum?id=B1xJAsA5F7>. 1
- 149 [8] Wengong Jin, Regina Barzilay, and Tommi Jaakkola. Multi-objective molecule generation
150 using interpretable substructures. In *International Conference on Machine Learning*, pages
151 4849–4859. PMLR, 2020. 1, 4, 6, 7
- 152 [9] Yibo Li, Liangren Zhang, and Zhenming Liu. Multi-objective de novo drug design with
153 conditional graph generative model. *Journal of cheminformatics*, 10(1):1–24, 2018. 6
- 154 [10] Łukasz Maziarka, Agnieszka Pocha, Jan Kaczmarczyk, Krzysztof Rataj, Tomasz Danel, and
155 Michał Warchoń. Mol-cyclegan: a generative model for molecular optimization. *Journal of*
156 *Cheminformatics*, 12(1):1–18, 2020. 1
- 157 [11] AkshatKumar Nigam, Pascal Friederich, Mario Krenn, and Alán Aspuru-Guzik. Augmenting
158 genetic algorithms with deep neural networks for exploring the chemical space. In *8th Interna-*
159 *tional Conference on Learning Representations, ICLR 2020, Addis Ababa, Ethiopia, April 26-30,*
160 *2020*. OpenReview.net, 2020. URL <https://openreview.net/forum?id=H1lmyRNFvr>. 4,
161 7
- 162 [12] AkshatKumar Nigam, Robert Pollice, and Alan Aspuru-Guzik. Janus: Parallel tempered
163 genetic algorithm guided by deep neural networks for inverse molecular design. *arXiv preprint*
164 *arXiv:2106.04011*, 2021. 4, 7
- 165 [13] Marco Podda, Davide Bacciu, and Alessio Micheli. A deep generative model for fragment-based
166 molecule generation. In *International Conference on Artificial Intelligence and Statistics*, pages
167 2240–2250. PMLR, 2020. 1
- 168 [14] John Schulman, Filip Wolski, Prafulla Dhariwal, Alec Radford, and Oleg Klimov. Proximal
169 policy optimization algorithms. *arXiv preprint arXiv:1707.06347*, 2017. 6
- 170 [15] Martin Simonovsky and Nikos Komodakis. Graphvae: Towards generation of small graphs
171 using variational autoencoders. In *International conference on artificial neural networks*, pages
172 412–422. Springer, 2018. 1
- 173 [16] Martin Stolle and Doina Precup. Learning options in reinforcement learning. In *International*
174 *Symposium on abstraction, reformulation, and approximation*, pages 212–223. Springer, 2002.
175 1

- 176 [17] Richard S. Sutton, Doina Precup, and Satinder Singh. Between mdps and semi-mdps: A
 177 framework for temporal abstraction in reinforcement learning. *Artificial Intelligence*, 112(1):
 178 181–211, 1999. 1
- 179 [18] Aäron van den Oord, Oriol Vinyals, and Koray Kavukcuoglu. Neural discrete representation
 180 learning. In Isabelle Guyon, Ulrike von Luxburg, Samy Bengio, Hanna M. Wallach, Rob Fergus,
 181 S. V. N. Vishwanathan, and Roman Garnett, editors, *Advances in Neural Information Processing
 182 Systems 30: Annual Conference on Neural Information Processing Systems 2017, December 4-9,
 183 2017, Long Beach, CA, USA*, pages 6306–6315, 2017. URL [https://proceedings.neurips.
 184 cc/paper/2017/hash/7a98af17e63a0ac09ce2e96d03992fbc-Abstract.html](https://proceedings.neurips.cc/paper/2017/hash/7a98af17e63a0ac09ce2e96d03992fbc-Abstract.html). 1
- 185 [19] Yutong Xie, Chence Shi, Hao Zhou, Yuwei Yang, Weinan Zhang, Yong Yu, and Lei Li.
 186 {MARS}: Markov molecular sampling for multi-objective drug discovery. In *International
 187 Conference on Learning Representations*, 2021. URL [https://openreview.net/forum?
 188 id=kHSu4ebxFXY](https://openreview.net/forum?id=kHSu4ebxFXY). 1, 4, 6, 7
- 189 [20] Jiakuan You, Bowen Liu, Zhitao Ying, Vijay S. Pande, and Jure Leskovec. Graph convolutional
 190 policy network for goal-directed molecular graph generation. In Samy Bengio, Hanna M.
 191 Wallach, Hugo Larochelle, Kristen Grauman, Nicolò Cesa-Bianchi, and Roman Garnett, editors,
 192 *Advances in Neural Information Processing Systems 31: Annual Conference on Neural
 193 Information Processing Systems 2018, NeurIPS 2018, December 3-8, 2018, Montréal, Canada*,
 194 pages 6412–6422, 2018. URL [https://proceedings.neurips.cc/paper/2018/hash/
 195 d60678e8f2ba9c540798ebbd31177e8-Abstract.html](https://proceedings.neurips.cc/paper/2018/hash/d60678e8f2ba9c540798ebbd31177e8-Abstract.html). 1

196 A Appendix

197 A.1 Reinforcement learning algorithm details

198 We detail the specifics of our reinforcement learning algorithm in [Algorithm 1](#). To bias the initial
 199 state distribution to favor molecules that can derive more novel high quality molecules, we keep
 200 an upper-confidence-bound (UCB) score for each initial molecule in the frontier F . We record the
 201 number of times we initiate a search $N(x, t)$ from a molecule $x \in F$, and the number of molecules
 202 qualified for adding to G that are found in episodes starting from x : $R(x, t)$. Here $t = \sum_{x \in \rho_0} N(x)$
 203 is the total number of search episodes. The UCB score of the initial molecule m is calculated by:

$$UCB(x, t) = \frac{R(x, t)}{N(x, t)} + \frac{\sqrt{\frac{3}{2} \log(t + 1)}}{N(x, t)} \quad (1)$$

204 The probability of a molecule in the initialization set being sampled as the starting point of a new
 205 episode is then computed by a softmax over the UCB scores: $p_{init}(x, t + 1) = \frac{\exp(UCB(x, t))}{\sum_{x \in I} \exp(UCB(x, t))}$.

206 We train our RL policy using the Proximal Policy Optimization (PPO, Schulman et al. 14) algorithm.
 207 We find the RL training robust despite both the reward function r and the initial state distribution
 208 ρ_0 are non-stationary (i.e., changing during the course of RL training). We construct the initial set
 209 of molecules for our search algorithm from the rationales extracted from [8]. These rationales are
 210 obtained through a sampling process, Monte Carlo Tree Search (MCTS), on the active molecules
 211 that tries to minimize the size of the rationale subgraph, while maintaining their inhibitory properties.
 212 Rationales for multi-property tasks (GSK3 β +JNK3) are obtained by combining the rationales for
 213 single-property tasks.

214 A.2 Experimental setup

215 **Datasets.** The dataset, originally extracted from ExCAPE-DB, contains 2665 and 740 actives
 216 for GSK3 β and JNK3 respectively. Each target also contains 50,000 negative ligand molecules.
 217 Following previous works [9, 8, 19], we adopt the same strategy of using a random forest trained on
 218 these datasets as the oracle property predictor. QED is a quantitative score that assesses the quality
 219 of a molecule through comparisons of its physicochemical properties to approved drugs. SA is a
 220 score that accounts for the complexity of the molecule in the context of easiness of synthesis, thereby
 221 providing an auxiliary metric for the feasibility of the compound as a drug candidate.

Algorithm 1 Molecule Search through **F**ragment-based **S**equential **T**ranslation (FaST)

```
1: Input:  $N$  is the desired number of discovered new molecules
2: Input:  $I$  is the initial set of molecules
3: Input:  $D$  is the decoder pretrained using the VQ-VAE
4: Input:  $T : X \rightarrow \{0, 1\}$  is the episode termination criterion function given an input molecule  $x$ 
5: Input:  $C : X \rightarrow \{0, 1\}$  is a function that returns 1 if the input  $x$  satisfies the desired properties.
6: Let  $G = \emptyset$  be the discovered set of molecules
7: Let  $F = I \cup G$  be the frontier where search is initialized from
8: Let  $t = 0$  be the number of episodes
9: while  $|G| \leq N$  do
10:   Let  $t = t + 1$ 
11:   Update  $UCB(x, t) \forall x \in F$  according to Equation (1)
12:   Sample initial molecule  $x_0 = (V, E)$  from  $p_{init} = \sigma[UCB(x, t)] \forall x \in F$ 
13:   Let  $x = x_0$ 
14:   while  $T(x) = 0$  do
15:     Sample action type  $a$  from  $p_{action} = \sigma[MLP(h_x)] \in \{\text{ADD}, \text{DELETE}\}$ 
16:     if  $a = \text{ADD}$  then
17:       Sample  $v_{add}$  from  $p_{add}(v) = \sigma[MLP(h_v)] \forall v \in V$ 
18:       propose fragment encoding as action  $f(x, v_{add}) = MLP([h_x; h_{v_{add}}])$ 
19:       Decode fragment  $y = D(f(x, v_{add}))$ 
20:       Add fragment  $y$  to molecule:  $x \leftarrow x + y$ 
21:     else
22:       Sample  $e$  from  $p_{del}(e) = \sigma[MLP(h_{e_{ij}})] \forall e \in E$ 
23:       Let  $y$  be the fragment designated by  $e$ , delete fragment  $x \leftarrow x - y$ 
24:     if  $C(x) = 1$  then
25:        $G \leftarrow G \cup \{x\}$ 
26:        $F \leftarrow I \cup G$ 
```

222 **Molecular Fragments** are extracted from molecules in the ChEMBL database [4]. For each molecule,
223 we randomly sample fragments by extracting subgraphs that contain 10 or fewer atoms that have a
224 single bond attachment to the rest of the molecule. We then use a VQ-VAE to encode these fragments
225 into a meaningful latent space. The use of molecular fragments simplifies the search problem, while
226 the variable-sized fragment distribution maintains the reachability of most molecular compounds.
227 Because our search algorithm ultimately uses the latent representation of the molecules as the action
228 space, we find that using a VQ-VAE with a categorical prior instead of the typical Gaussian prior
229 makes RL training stable and provides performance gains.

230 **Evaluation metrics.** Following previous works, we evaluate our generative model on three target
231 metrics, success, novelty and diversity. 5,000 molecules are generated by the model, and the metric
232 scores are computed as follows: **Success** measures the proportion of generated molecules that fit
233 the desired properties. For inhibition of GSK3 β and JNK3, this is a score of at least 0.5 from the
234 pretrained predictor. QED has a target score of $\geq .6$ and SA has a target score of ≤ 4 . **Novelty**
235 measures how different the generated molecules are compared to the set of actives in the dataset, and
236 is the proportion of molecules whose fingerprint similarity is at most .4 to any molecule in the active
237 set. **Diversity** measures how different the generated molecules are compared to each other. Here,
238 diversity is computed as an average of pairwise fingerprint similarity across all generated compounds.

239 **Baseline methods.** **Rationale-RL** [8] extracts rationales of the active molecules and then uses
240 RL to train a completion model that add atoms to the rationale in a sequential manner to generate
241 molecules satisfying the desired properties. **GA+D & JANUS** [11, 12] are two genetic algorithms
242 that use random mutations of SELFIES strings to generate promising molecular candidates; JANUS
243 leverages a two-pronged approach, accounting for mutations towards both exploration and exploita-
244 tion. **MARS** [19] uses Markov Chain Monte Carlo (MCMC) sampling to iteratively build new
245 molecules by adding or removing fragments, and the model is trained to fit the distribution of the
246 active molecules. We additionally include a baseline **MARS+Rationale** that initialize the MARS
247 algorithm with the same starting initial rationale set used in Rationale-RL and our method in order to

248 provide better comparisons of the methods. Where possible, we use the numbers from the original
249 corresponding paper.